Towards Contactless Estimation of Electrodermal Activity Correlates

Mayur J. Bhamborae[1], Philipp Flotho[1], Adrian Mai[1], Elena N. Schneider[1], Alexander L. Francis[2] and Daniel J. Strauss[1,3] .

Abstract— **This paper presents a proof-of-concept for contactless and nonintrusive estimation of electrodermal activity (EDA) correlates using a camera. RGB video of the palm under three different lighting conditions showed that for a suitably chosen illumination strategy the data from the camera is sufficient to estimate EDA correlates which agree with the measurements done using laboratory grade physiological sensors. The effects we see in the recorded video can be attributed to sweat gland activity, which inturn is known to be correlated with EDA. These effects are so pronounced that simple pixel statistics can be used to quantify them. Such a method benefits from advances in computer vision and graphics research and has the potential to be used in affective computing and psychophysiology research where contact based sensors may not be suitable.**

Index Terms— **electrodermal activity, non-intrusive, camera-based, remote psychophysiology, affective computing**

I. Introduction

Electrodermal activity (EDA) refers to changes in the electrical properties of the skin. These changes are attributed to variations in eccrine sweat gland activity which in turn is modulated by the sympathetic nervous system. EDA has been shown to have strong correlation with emotional arousal and the affective state of a person and is consequently a commonly used measure of the same in psychophysiological and neurophysiological studies [1], [2]. This has lead to EDA being used in several applications across various disciplines, both clinical and non-clinical.

Different methods can be used to measure EDA; all of which require electrodes that make contact with skin. Thus making them **noninvasive but intrusive** methods. The electrodes, which measure skin conductance, are generally placed at locations with high density of eccrine sweat glands, such as the palmar surface of the hand. Detailed information on how EDA is measured can be found in [1]. Recording EDA using electrodes requires the subject to keep the hand relatively stable for the duration of the recording as it is quite sensitive to motion. This limits its use to controlled environments. Although wearable EDA devices have become popular in recent years they may still be unsuitable in situations where having contact based sensors are undesirable. For instance, in automotive applications, EDA is known to correlate with motion sickness [3] and driver stress [4]. In such cases, it is desirable to have a system that is able to remotely estimate the EDA.

Visual computing based methods are no novelty to psychophysiological and affective computing research. Emotion and affective state can be communicated using facial expressions and body gesture among other modalities [5]. There exists rich literature on the applications of facial expressions and body gesture in affective computing such as in [6], [7]. Despite significant improvements in camera and computer vision technologies, researchers still prefer using physiological data such as EDA because data from cameras, due to different factors such as errors in tracking and detection and large inter-subject variations, can often be ambiguous and lacks in quality compared to raw signals from physiological sensors. EDA continues to be the gold standard in psychophysiological research.

Thermography is another visual computing based tool that is popular among psychophysiology and affective computing researchers. This is motivated by the fact that the primary function of eccrine sweat glands is actually thermoregulation which causes changes in skin conductance due the nature of its function. Eccrine sweat gland activity is also shown to be modulated by affect and emotions [1], [8]. Among the many psychophysiological studies that use thermography, some of the most interesting to us are the works of Shastri et al. [9] and Krzywicki et al. [10]. In [9] we see the possibility of detecting peripheral sympathetic responses using only thermographic imaging of the face and in [10] they use high resolution thermography to quantify eccrine sweat gland activity which was shown to be positively correlated to the skin conductance response. One issue with thermography is that high resolution thermal cameras are relatively expensive compared to their visible (RGB) or near-infrared (NIR) counterparts and may not be suitable in all situations. A state of the art survey on the use of thermography in psychophysiological research can be found in [11].

In this work we show what is to our knowledge for the first time (early 2020), that correlates of EDA can be estimated nonintrusively using commercially available RGB sensors. Our hypothesis for this work is that EDA variations due to sweat gland activity can be estimated using a camera monitoring the skin. Such image based approaches can benefit from recent advances in computer vision and graphics research such as in [12], [13], [14]. Our setup uses a machine vision RGB camera and three white LED spotlights to illuminate the scene (in our case, the left palm) from three different angles. We also record the EDA using laboratory-grade sensors as the ground truth. An interesting observation

[1] Systems Neuroscience and Neurotechnology Unit (Visual Computing Lab), Neurocenter, Saarland University Hospital, Homburg/Saar, Germany. (mayur.bhamborae@uni-saarland.de)

[2] Speech Perception and Cognitive Effort (SPACE) Lab, Purdue University, Lyles-Porter Hall, 715 Clinic Drive, West Lafayette, IN, USA

[3] Key Numerics GmbH , Saarbrücken, Germany.

from the recorded data is that the effects of strong EDA changes are visible in the video with minimal processing.

The rest of this paper describes our setup, measurement procedure and discusses the preliminary findings of our experiments. Specifically, Section II has the description of the setup and the measurement paradigm. Section III discusses the results of the experiments and the evaluation of the gathered data and in Section IV, we conclude this paper after briefly mentioning the future direction of this study.

II. Materials and Methods

A. Imaging System

We use a machine vision camera with a 1.3 Megapixel (1280×1024) CMOS RGB sensor with 24 bits per pixel (8 bits per for each R, G and B channel) and a 35mm F1.4 lens. We use three commercially available DMX512 controllable 15 W white LED spotlights for the illumination. The spotlights are set at different angles, therefore each light strongly illuminates a different region of the palm. As we see in the left column of Figure 2, light 1 strongly illuminates the hypothenar region, light 2 the middle of the palm and light 3 illuminates the thenar region. Figure 1 shows the lights and camera arrangement we use. We record a video of the subject's palm with a sequence of three time multiplexed light sources. Since the video capture rate is around 30 Hz, the scene is illuminated with one of the three lights every 10th of a second.

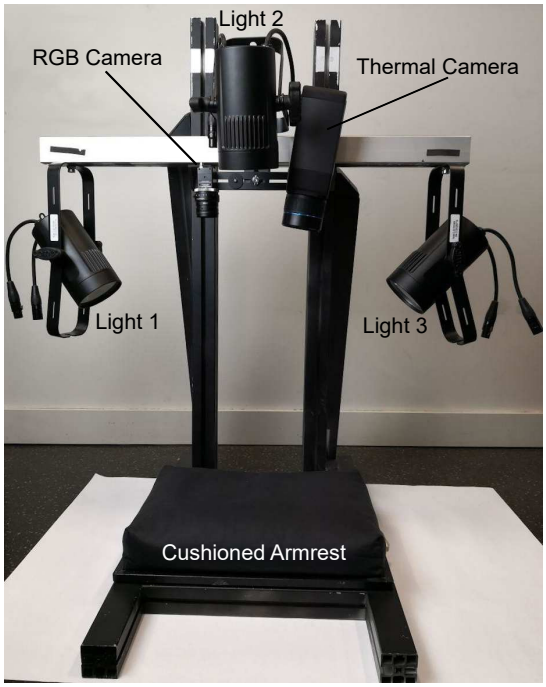

Fig. 1: Our setup records a time-multiplexed video with three different lighting conditions. Light 1 illuminates the hypothenar region, light 2 the middle of the palm and light 3 illuminates the thenar region.

B. EDA Measurement and Data Processing

The EDA measurement setup consists of EDA sensors and a biosignal amplifier. The device measures exosomatic skin conductance using a constant DC voltage of approximately 400 mV with a sampling frequency of 512 Hz. The electrodes are placed on proximal phalanges of the index and middle fingers of the non-dominant hand (in this case left) and fixed with hook-and-loop fasteners.

The EDA data is then bandpass filtered with cut-off frequencies 0.01 and 40 Hz to remove low frequency noise and include high frequency phasic activity.

C. Measurement Paradigm

To minimize the impact of outside light, the measurements are done in a darkened environment. The image acquisition system was started simultaneously with the EDA data recorder. The overall duration of the measurement is about twenty minutes and follows a paradigm designed to elicit strong electrodermal responses using audio, video and physical stimuli. This measurement protocol was approved by the Medical Chamber of Saarland (Ärztekammer des Saarlandes).

At the very beginning of the measurement, a five minute long calming video of a creek was shown. This was done to get the baseline measurement. The first task was to perform three repetitions of a version of the Valsalva maneuver, which is a commonly used maneuver to evaluate the functioning of the autonomic nervous system and results in strong electrodermal activity. Each maneuver lasts 10 seconds followed by a recovery phase (RP) of 1 minute. Next, the subject was presented with visual stimuli from the International Affective Picture System (IAPS) [15]. Following this was a mix of pleasant and unpleasant auditory stimuli from International Affective Digitized Sounds (IADS -2) [16]. All stimuli and tasks had appropriate breaks between them.

D. Image Data Processing

Each frame in the video is an image of the scene with only one of the three spotlights active. Visual inspection of the recorded video shows that the number of specular points (shiny pixels) is higher in some frames than others. In Section III we show that these frames correspond to strong changes in the electrodermal activity. The position and intensity of such specular points depends on the surface normal (which is a function of the curvature of the palm), the viewing angle and the angle of illumination, therefore it becomes difficult to establish a good mapping of points between the frames with different illumination conditions. To enable reliable analysis, we use an optical flow based approach to stabilize the video frames. We do this separately for each lighting angle. We start with light 1, and initialize the flow for light 2 and light 3 by linearly interpolating the displacements of light 1. This linear assumption holds true for the almost the entire recording as the subject's hand was relatively stable for the duration of the measurement. We remove any residual motion from light 2 and light 3 with

explicit motion compensation. We carry out all our analyses and evaluations on these motion compensated frames.

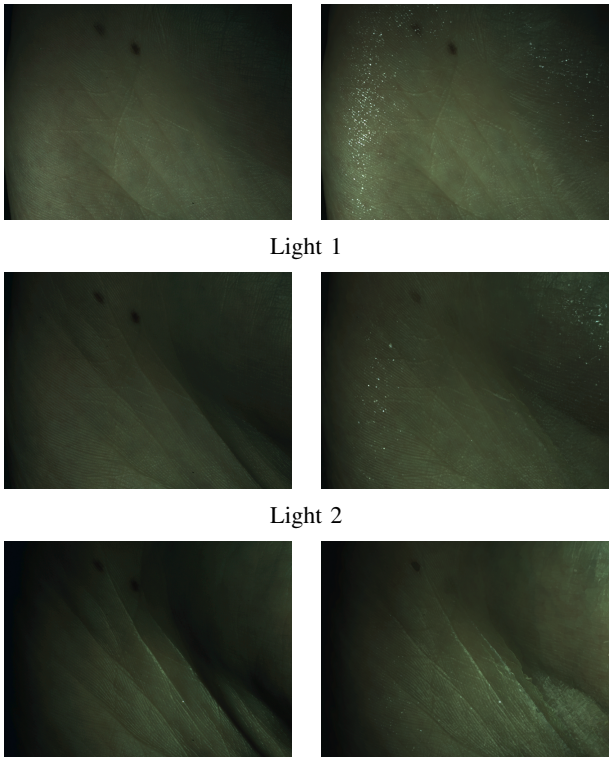

Fig. 2: *Left*: Consecutive frames from time multiplexed video capture with three different lighting conditions during the baseline measurement. *Right*: Maximum intensity projection of the stabilized video in the temporal dimension.

III. Evaluations and Results

For our preliminary analysis, we split the video into three independent sets of frames, each set associated with one of the three light sources. In Section II-D we mention briefly that the number of specular (shiny) pixels is higher at certain points in time. We quantify the occurrence of specular pixels by their count, which we shall call *Specular Pixel Count*. The location of increased specular pixels depends on the direction of the light source associated with the frame. Although the lights are adjusted to uniformly illuminate the palm, we see higher specular pixel count in the hypothenar region of the palm due to the light 1, the middle of the palm due to light 2 and the thenar region due to light 3. This is due to the natural geometry of the palm, which is a not a flat surface but has a curvature. We identify these pixels in the Hue Saturation Value (HSV) color space. This gives us three values per pixel: Hue (H), Saturation (S) and Value (V). Specular pixels have low saturation (S) and high value (V). We consider all those pixels with $S < 0.4$ and $V > 0.5$ as being specular. These values are chosen to maximize the correctly detected specular pixels and minimize false detections due to noise.

The specular effects are strongest in the hypothenar region and therefore for the preliminary analysis we only consider the subset of frames that are associated with light 1, that is, frames where the hypothenar region is most strongly illuminated. In Figure 3 we show a comparison of the specular pixel count from the hypothenar region with the skin conductance values from the EDA measurements. We see that there is an increase in specular pixel count at those points in time where there are strong changes in the SC values. This is in agreement with the fact that changes in skin conductance occur due to variations in sweat gland activity. The increase in specular pixel count can be attributed to the formation and quick evaporation of tiny sweat droplets, which inturn cause noticeable changes in the appearance of skin in the video.

Looking at Figure 3, not only do we see correlating activity for the important events of the experiment, but there are many small peaks of activity in the EDA with a correlate in the specular pixel count. The sweat droplet formation and evaporation effects are quick enough such that we are able to identify some phasic activity from this relatively unprocessed data. For instance, we see a sharp increase in the specular pixel count at those points which mark the beginning of a section (such as the onset of the Valsalva maneuvers) which is also marked by a surge in skin conductance. Interestingly, a quicker drop in the specular pixel count can also be seen as the skin conductance levels gradually return to the baseline.

In last section, marked by the end of the paradigm, we see heightened electrodermal activity due to the subject being aroused after being informed about the completion of the recording. We see these changes in the specular pixel count as well. This is quite interesting as this was initially not expected at all.

Our preliminary analysis only considers those frames when light 1 was active because the aforementioned effects are best visible in the hypothenar region. While similar effects can be also be seen in other regions of the palm (see right column of Figure 2), many frames from the light 2 and light 3 subsets had to be discarded due to occlusions and shadows caused by movements of the thumb.

IV. Conclusion and Future Work

In this paper we showed that is possible to estimate correlates of EDA using RGB cameras. While it is known, that changes in the skin properties can be monitored, we did not expect the effects in the video to be strong enough to be visible to the naked eye and to be easily quantifiable with a combination of motion compensation and simple pixel statistics.

Our findings from this pilot study serve as valuable inputs for the next steps in this direction. In a larger follow up study, we are currently investigating how common the effects are and whether we can find a relationship of the observed specular reflections and the EDA signal that is valid for a larger study population. Looking at the preliminary results, the reason for the different dynamics in specular reflection and EDA is a candidate for further analysis.

While for the data presented here, simple pixel statistics were sufficient, subjects with smaller responses in the video

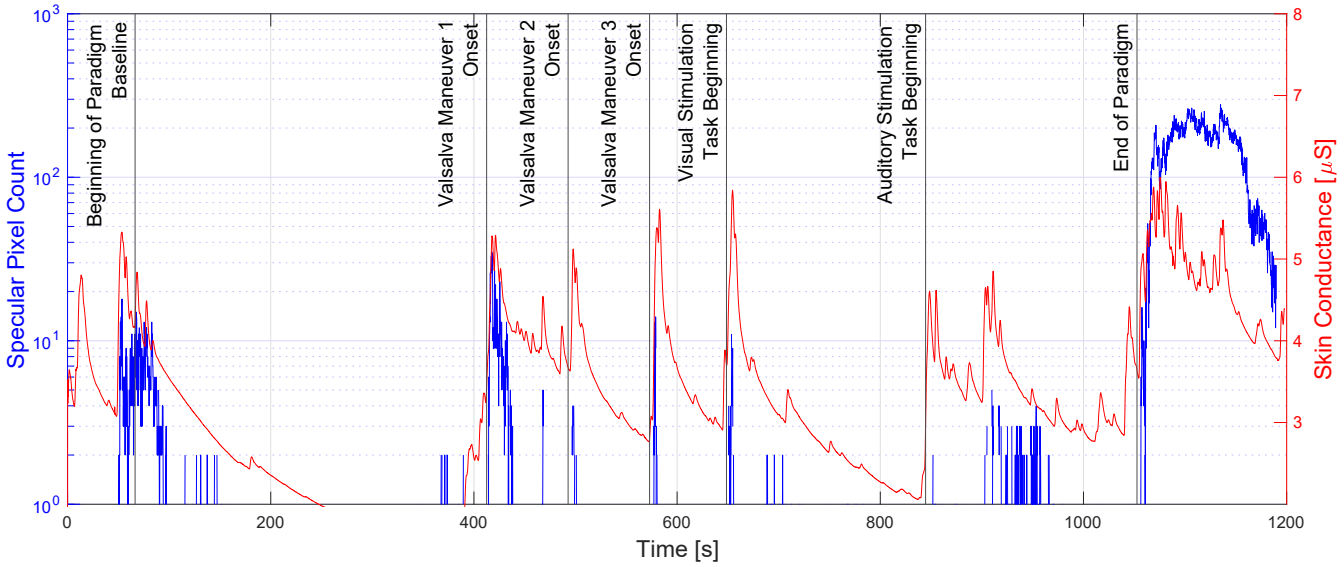

Fig. 3: Comparison of skin conductance (in red) measured using laboratory-grade EDA sensors and the specular pixel count (in blue) due to Light 1 computed from the video frames. We clearly see an increase in the specular pixel count during the events of the experiment with heightened skin conductance levels. We also see many peaks in the specular pixel count which correlate with the skin conductance levels. The specular pixel count has been logarithmically scaled to adjust for the large activity towards the end of the experiment.

and more complicated conditions such as recordings from the face will require models from computer graphics which account for the layered nature of skin and the interaction of light with skin, such as [17], [13], [18] to obtain parameters which can be investigated for correlation with EDA. Such models would open the way for robust, contactless EDA measurements with the ultimate goal of EDA estimation from facial videos in a natural environment. This has the potential to unlock new areas where the results from affective EDA research can be applied and where contact based sensors are not suitable.

Acknowledgment

This work was partially funded by the German Federal Ministry of Transport and Digital Infrastructure (BMVI) in the framework of the kantSaar Project under grant 16AVF2129B.

References

[1] W. Boucsein, *Electrodermal activity: Second edition*. New York, NY, US: Springer Science + Business Media, 2012, vol. 9781461411260.

[2] M. E. Dawson, A. M. Schell, and D. L. Filion, "The electrodermal system," in *Handbook of Psychophysiology*, J. T. Cacioppo, L. G. Tassinary, and G. G. Berntson, Eds. Cambridge University Press, 2007, ch. 8, pp. 200–223.

[3] L. A. Warwick-Evans, R. E. Church, C. Hancock, D. Jochim, P. H. Morris, and F. Ward, "Electrodermal activity as an index of motion sickness." *Aviation, Space, and Environmental Medicine*, vol. 58, no. 5, pp. 417–423, 1987.

[4] J. A. Healey and R. W. Picard, "Detecting stress during real-world driving tasks using physiological sensors," *IEEE Transactions on intelligent transportation systems*, vol. 6, no. 2, pp. 156–166, 2005.

[5] R. W. Picard, *Affective computing*. MIT press, 2000.

[6] T. Baltrušaitis, D. McDuff, N. Banda, M. Mahmoud, R. e. Kaliouby, P. Robinson, and R. Picard, "Real-time inference of mental states from facial expressions and upper body gestures," in *Face and Gesture 2011*, March 2011, pp. 909–914.

[7] H. Gao, A. Yüce, and J. Thiran, "Detecting emotional stress from facial expressions for driving safety," in *2014 IEEE International Conference on Image Processing (ICIP)*, Oct 2014, pp. 5961–5965.

[8] R. W. Picard, S. Fedor, and Y. Ayzenberg, "Multiple arousal theory and daily-life electrodermal activity asymmetry," *Emotion Review*, vol. 8, no. 1, 2016.

[9] D. Shastri, A. Merla, P. Tsiamyrtzis, and I. Pavlidis, "Imaging facial signs of neurophysiological responses," *IEEE Transactions on Biomedical Engineering*, vol. 56, no. 2, pp. 477–484, 2009.

[10] A. T. Krzywicki, G. G. Berntson, and B. L. O'Kane, "A non-contact technique for measuring eccrine sweat gland activity using passive thermal imaging," *International Journal of Psychophysiology*, vol. 94, 2014.

[11] Y. Cho and N. Bianchi-Berthouze, "Physiological and affective computing through thermal imaging: A survey," 2019.

[12] P. Hanrahan and W. Krueger, "Reflection from layered surfaces due to subsurface scattering," in *Proceedings of the 20th Annual Conference on Computer Graphics and Interactive Techniques*, ser. SIGGRAPH '93. Association for Computing Machinery, 1993.

[13] A. Ghosh, T. Hawkins, P. Peers, S. Frederiksen, and P. Debevec, "Practical modeling and acquisition of layered facial reflectance," *ACM Trans. Graph.*, vol. 27, no. 5, Dec. 2008.

[14] P. Debevec, T. Hawkins, C. Tchou, H.-P. Duiker, W. Sarokin, and M. Sagar, "Acquiring the reflectance field of a human face," in *Proceedings of the 27th Annual Conference on Computer Graphics and Interactive Techniques*, ser. SIGGRAPH '00. USA: ACM Press/Addison-Wesley Publishing Co., 2000, p. 145–156.

[15] P. J. Lang and M. M. Bradley, "International affective picture system (IAPS): Technical manual and affective ratings," University of Florida, Gainesville, FL, Tech. Rep., 2008.

[16] M. M. Bradley and P. J. Lang, "The international affective digitized sounds (2nd edition; IADS-2): Affective ratings of sounds and instruction manual," University of Florida, Gainesville, FL, Tech. Rep., 2007.

[17] A. Krishnaswamy and G. V. G. Baranoski, "A Biophysically-Based Spectral Model of Light Interaction with Human Skin," *Computer Graphics Forum*, vol. 23, no. 3, pp. 331–340, 2004.

[18] T. Weyrich, W. Matusik, H. Pfister, B. Bickel, C. Donner, C. Tu, J. McAndless, J. Lee, A. Ngan, H. W. Jensen, and M. Gross, "Analysis of human faces using a measurement-based skin reflectance model," *ACM Trans. on Graphics (Proc. SIGGRAPH 2006)*, vol. 25, no. 3, pp. 1013–1024, 2006.